Composites Part B 194 (2020) 108061

Contents lists available at ScienceDirect

Composites Part B

journal homepage: www.elsevier.com/locate/compositesb

Direct ink writing of surface-modified flax elastomer composites

Yizhou Jiang, Jevon Plog, Alexander L. Yarin **, Yayue Pan *

Department of Mechanical and Industrial Engineering, University of Illinois at Chicago, 842 W. Taylor St., Chicago, IL, 60607, USA

ARTICLE INFO

Keywords:
Flax
Direct ink writing
Surface modification
Natural fiber
Sonication

ABSTRACT

Compared with synthetic fibers, natural fibers exhibit high specific mechanical strength, excellent thermal and acoustic insulation, and super biodegradability. These characteristics made them potential materials for green, sustainable, and inexpensive manufacturing of the next-generation composite components. This work focuses on addressing the material extrusion challenge in 3D printing natural fibers using direct ink writing technique. Flax fiber, a common natural fiber, is studied. Influence of the layered structure of the flax fiber on the printability in direct ink writing process is investigated. Techniques. It is found that the outer layer of the fiber can be controllably removed by the sonication process and the processed fiber can be dispersed uniformly in the elastomer to form a homogeneous ink, which overcomes the tip clogging issue in extrusion-based 3D printing techniques. To understand and quantify the influence, rheological properties are characterized. Additionally, the printability is investigated. Furthermore, mechanical behaviors of the 3D printed flax-fiber elastomer composites are analyzed. It was found that with an addition of only 0.2 wt% surface-modified flax fibers, the tensile properties could be increased over 100%, which is comparable to or even higher than other synthetic fiber-based composites with much higher fiber loading fractions. The findings in this study indicate a novel and sustainable method to engineer composites using direct ink writing technique. The high degree of property tunability and material biocompatibility indicate great promise of applications of the 3D printed fiber-elastomer composites in many fields, such as soft robotics, biomedical devices, and flexible wearable electronics.

1. Introduction

Silicone-based elastomers, such as polydimethylsiloxane (PDMS), have superior elasticity, biocompatibility, and optical transparency [1,2]. A broad range of applications has been demonstrated in bioengineering [3], flexible and wearable electronics [4]. Despite the superior intricate properties of elastomers and their wide applications, researchers also started to investigate functional fillers for producing elastomer composites with new material functionalities [5,6]. Carbon fibers [7], glass fibers [8], and metal particles [9] embedded in elastomer composites have been recently reported. However, those functional fillers are usually made from unsustainable petroleum. They are not biodegradable and can cause serious disposal/recycling problems in the environment.

Recently, the use of natural fibers instead of synthetic fibers in composite materials attracted significant attention of research community. Extensive studies on natural fibers, including sisal [10], jute [11], and flax [12] demonstrated the potential for a green, sustainable and inexpensive components for the next-generation composite materials. These natural fibers exhibit high specific mechanical strength, excellent thermal and acoustic insulation, as well as good biodegradability [13,14]. In contrast to relatively rigid synthetic fibers, natural fibers also offer excellent flexibility and softness, which make them ideal for many applications such as soft robotics and medical engineering [15,16].

Specifically, flax (Linum usitatissimum) is one of the commonly used natural fibers as reinforcement in composites [17]. Flax fibers are inexpensive and abundant in nature. It is one of the very first materials to be woven into textiles, which was found in graves in Egypt dating back to 5000 BC [18]. In recent years, Canada has been the largest producer and exporter of flax. Canada produced more than one million tons flax and exported approximately 60% to the EU, 30% to the USA, and 4% to Asia due to the increasing worldwide demand in linen market [19]. Some other leading producers of flax include France, Belgium and the Netherlands [20]. Climatic conditions in these regions and countries are suitable for growing and planting flax. The growing cycle of flax is usually short, with only 100 days between sowing and harvesting in

* Corresponding author.
** Corresponding author.
E-mail addresses: ayarin@uic.edu (A.L. Yarin), yayuepan@uic.edu (Y. Pan).

https://doi.org/10.1016/j.compositesb.2020.108061
Received 30 December 2019; Received in revised form 26 March 2020; Accepted 10 April 2020
Available online 16 April 2020

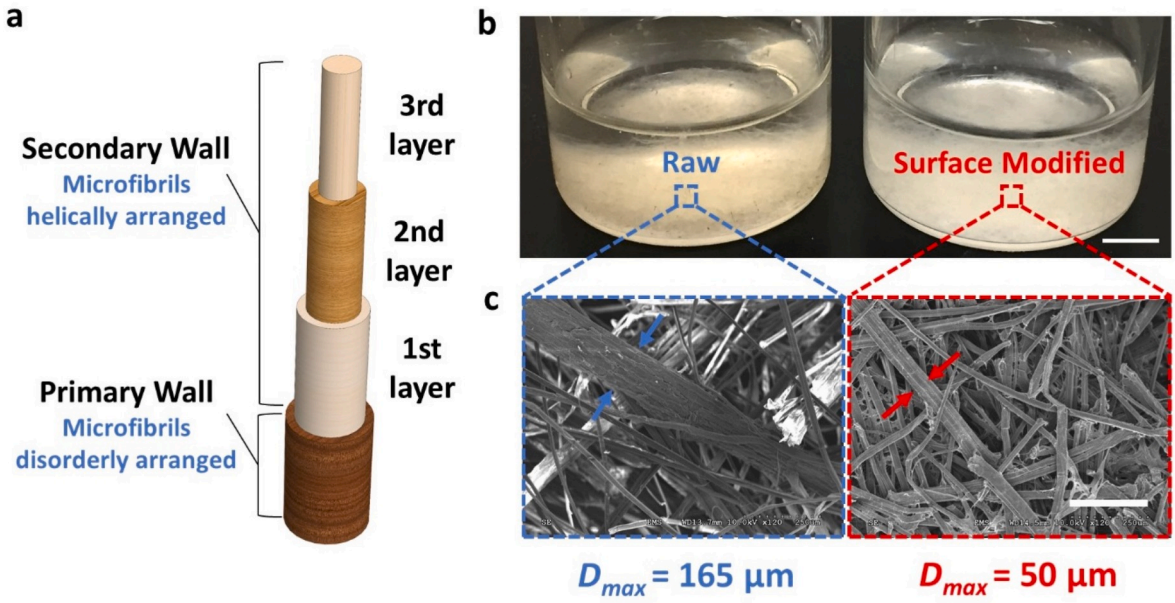

Fig. 1. Surface-modified short flax fibers. (a) Flax fiber layer-by-layer structure illustration. (b) Optical images of raw and surface-modified chopped flax fiber suspensions, scale bar = 5 mm. (c) SEM images of raw and surface-modified chopped flax fibers, scale bar = 250 µm.

some European regions [21].

Tensile properties of flax fibers are critical in fiber reinforced polymer composites. Charlet et al. tested single flax fiber using a universal tensile testing machine. It was found that the fibrils arrangement highly affects the tensile properties [22]. Garkhail et al. fabricated thermoplastic composites consists of flax fiber and polypropylene and investigated the influence of fiber length and fiber content on stiffness and strength [23]. It was revealed that the stiffness of the flax based composites is comparable to glass based composites, indicating that future research towards significant improvements in tensile and impact strength of these types of composites.

However, preparation of natural fibers like flax for matrix composites requires extensive efforts, due to substantial variations in fiber dimensions and orientations. Many approaches have been developed to prepare fibers in a more consistent and repeatable form, for ease in manufacturing and property control. For instance, it was reported that the alkali treatment of jute in Biopol composites can result in a 30% increase in bending strength [24]. It was proved that the storage modulus of short bamboo fiber-reinforced polypropylene composites could be increased by hybridization [25]. However, these material preparation methods involve complex chemical processes, and most of these composites were fabricated by subtractive manufacturing or injection molding, which have limited flexibility in terms of material manipulation and complicated object geometry.

Recent progress in additive manufacturing (AM) enables more advanced design and fabrication of fiber-embedded composites [26–28]. For example, carbon fiber-reinforced thermoplastic composites with improved mechanical properties have been fabricated by fused deposition modeling (FDM) in which the materials are extruded through a heated nozzle [29]. Fiber-filled epoxy resins and elastomers have also been demonstrated by direct ink writing (DIW) technique [30,31]. Specifically, in DIW process, the liquid-phase "ink" is dispensed through small nozzles under controlled flow rates and deposited along digitally defined paths to fabricate three-dimensional structures in a layer-by-layer way. In general, the printing mechanism of DIW can be pneumatic (air pressure) and mechanical (piston). Compared with other AM techniques, DIW widens the printable material range and achieves a higher manufacturing flexibility. However, studies reporting printing of natural fibers are very few. Printing heterogeneous natural-fiber-polymer composites by extrusion-based additive manufacturing technologies is challenging due to the poor dispersion of natural fibers, which usually have significant variation in dimensions. For extrusion-based AM approaches, one of the critical prerequisites is the ink homogeneity, to avoid the typical nozzle clogging issue.

In this study, for the first time, we report the direct ink writing of biocompatible surface-modified short flax elastomer composites with tunable mechanical properties. To enable the printability of the flax polymer composites in extrusion-based AM process, the flax fibers are surface modified into a consistent form by removing the outer layer of the raw fiber structure using the sonication approach. The mechanical properties of flax polymer composites are competitive or even better than synthetic fiber filled composites. The findings in this study indicate a novel and sustainable method to engineer composites using direct ink writing technique.

2. Material and methods

2.1. Microstructure of surface-modified flax fiber

Flax fibers have irregular polygonal cross-sections and a hollow structure, consisting of approximately 81% cellulose, 14% hemicellulose, 3% lignin, and 4% pectin [32]. The main structure of flax fibers consists of two walls, as shown in Fig. 1a. The first wall along the plant growth is a primary wall containing both cellulose and hemicellulose, with microfibrils disorderly arranged. The thickness of the primary wall is approximately 0.2 µm, according to the recent studies [33]. The secondary wall, which consists of another three layers (first, second, and third) is located inside the primary wall. The thickness of the second layer is usually more extensive than those of the first and third layers. It also contributes to the overall strength of the fiber. In this three-layer structure of the secondary wall, helically wound highly crystalline cellulose chains-structured microfibrils, have been observed. The microfibrils are formed by 30–100 cellulose molecule chain, oriented with an approximately 10° angle along the center axis of the fiber. The secondary wall contributes up to 70% to the fiber Young's modulus. Hence, a higher cellulose content can result in a higher tensile modulus.

As shown in Fig. 1b, we observed that the color of short flax fibers changed from brownish to white, and some dark brown particles (primary layer residues) were floating on top of the suspension during the sonication process after 3 h sonication process (300-Watt power setting).

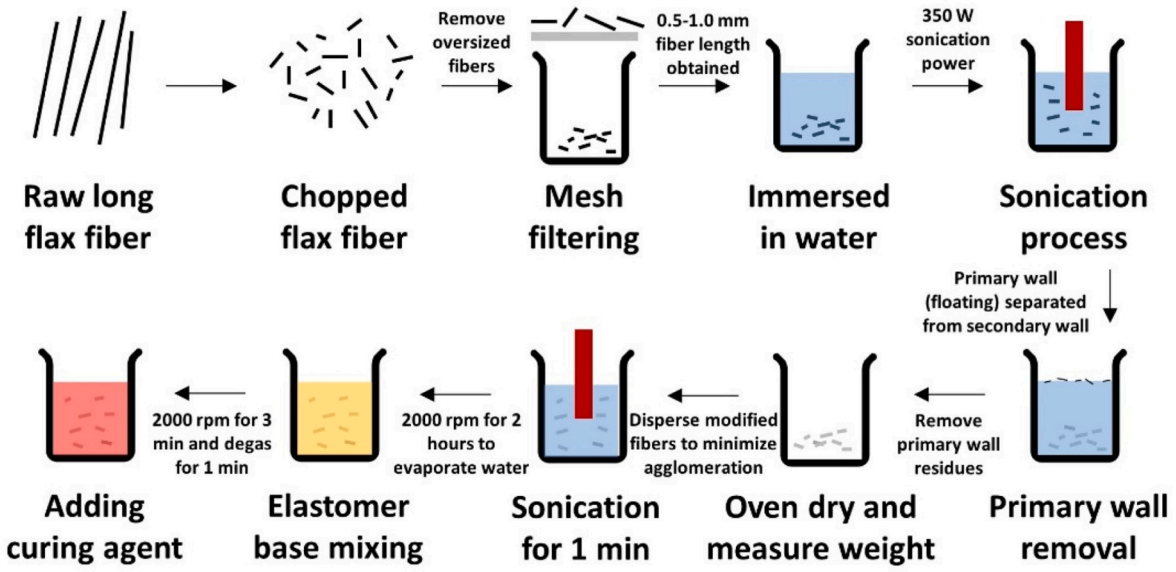

Fig. 2. Ink preparation process.

Fig. 1c shows the scanning electron microscopic images of the raw and surface-modified flax fibers. The sonication process mainly removed the primary wall of the raw flax fibers by moderate vibrations. Between each sonication period, those primary layer residues were filtered. The remaining surface-modified flax fibers (sonicated) became more consistent in dimensions upon the removal of these primary wall residues, which efficiently minimized the fiber agglomeration and made it possible to extrude fiber-dispersed inks without adding additional chemicals. In this study, D_{max} is defined as the maximum observed diameter of the bundled fiber under a microscope. Surface modified flax fiber shows much smaller D_{max}. D_{max} reduced from 165 μm to 50 μm by the surface modification process. Hence, the sonication process separated most large bundles of raw flax fibers, which further reduced the average fiber diameter to overcome the typical tip clogging issue in extrusion-based AM of fiber-embedded materials.

2.2. Surface-modified flax elastomer composite ink preparation

The typical tip clogging issue in extrusion-based AM process is caused by the fiber agglomeration [34]. Such agglomeration is usually due to the oversized fiber bundles in the composite ink, which tend to form large fiber blocks under the high shear stress during the material extrusion through the dispensing tip. To overcome it, those oversized fiber bundles need to be dispersed. The complete ink preparation process is shown in Fig. 2. Raw flax fibers with 20–200 μm diameter were first carefully chopped into short pieces. The length of the as-cut fibers mainly ranged from 0.5 mm to 2.0 mm. Afterward, 200 mg of short flax fibers were filtered by a copper mesh with 0.5 mm pores to further remove oversized flax fibers. The filtered flax fibers, together with 50 ml deionized water, were homogenized by a probe sonicator (QSonica Q500) at a 300-Watt power setting. The total sonication time was 3 h (30 min per sonication period, 6 periods in total). Between each sonication period, the mixture was cooled down to room temperature to avoid the overheating issue in probe sonication process.

After removing the primary wall of the raw flax fibers, the remaining surface-modified flax in deionized water suspension was dried at 90 °C in an oven overnight. The thoroughly dried surface-modified flax fibers were collected. In this study, to prepare the composite, Dow Sylgard 184 silicone elastomer was purchased and used as received. It is a two-component (base and curing agent, mix weight ratio 10:1), room temperature curing encapsulant. The 0.2 wt% and 0.5 wt% composites were prepared by adding 20 mg and 50 mg of surface-modified flax fibers to

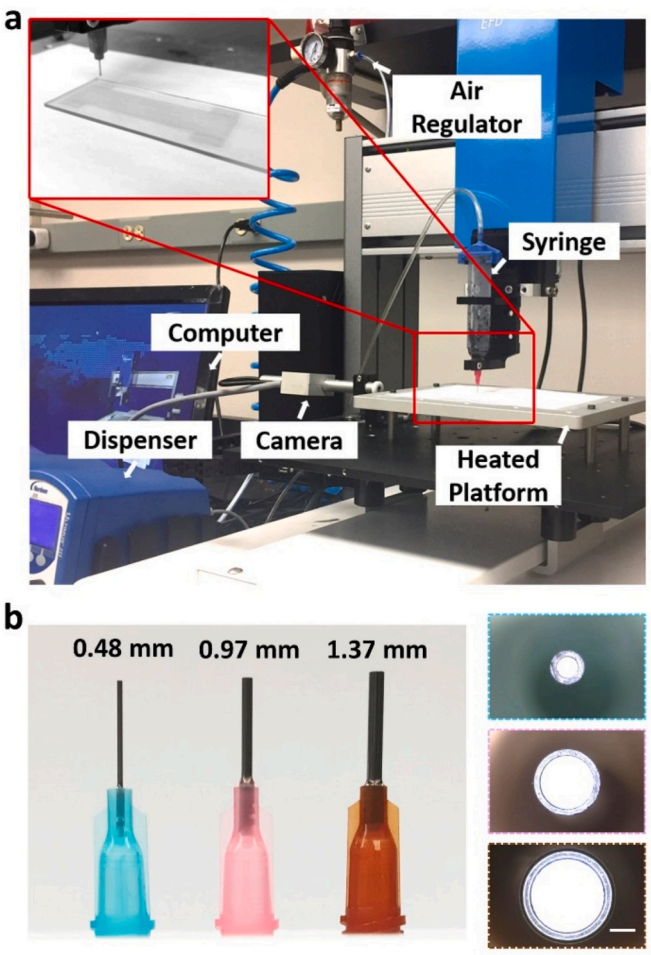

Fig. 3. DIW system setup and dispensing tips. (a) DIW system setup. (b) Dispensing needles, inner diameter ranges from 0.48 mm to 1.37 mm, scale bar = 0.50 mm.

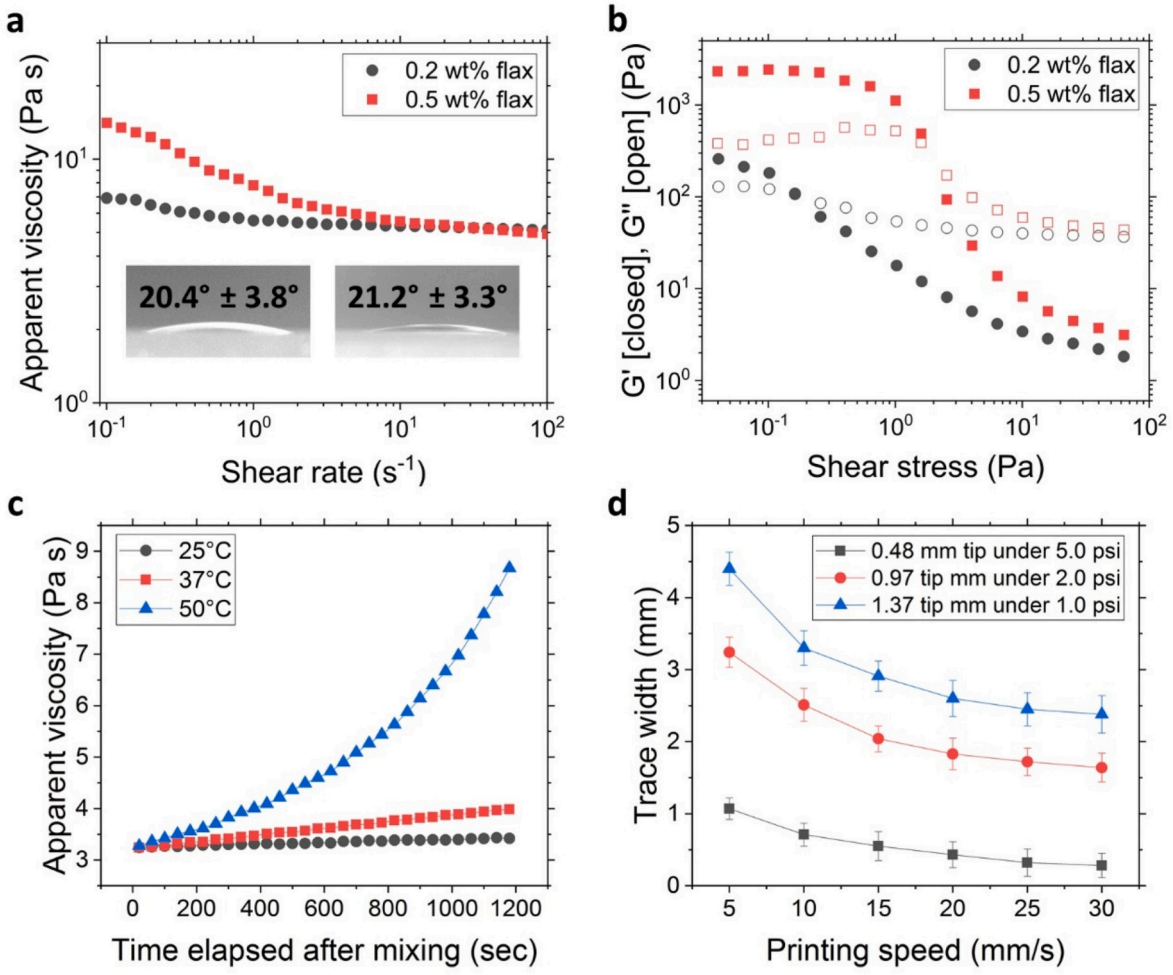

Fig. 4. Ink characterization of 0.2 wt% and 0.5 wt% flax composite inks. (a) Apparent viscosity measurements. (b) Elastic (G′) and loss (G′‘) moduli. (c) Temperature-dependent apparent viscosity changes of the elastomer after mixing. (d) Trace width of printed 0.2 wt% surface-modified flax elastomer composites under various dispensing tips and air pressure.

9.1 g elastomer base, separately. Both blends were mixed at 2000 rpm (AR-100, Thinky) for 30 min. Then, the blends were degassed (AR-100, Thinky) for 2 min. Afterward, they were blended with 0.9 g curing agent at 2000 rpm for 3 min before loading to a syringe barrel (Nordson EFD).

2.3. DIW system setup and fabrication process

Direct ink writing (DIW) is an additive manufacturing technique which was first developed for fabricating three-dimensional ceramic structures. Numerous applications including flexible electronic to soft functional devices have been demonstrated. Compared with other additive manufacturing techniques such as Fused Deposition Modeling (FDM) and Stereolithography (SLA), DIW enriches the printable materials to achieve a higher manufacturing flexibility. However, like many other extrusion-based AM process, printing natural fiber composites is challenging due to the large variations in fiber dimensions, causing tip clogging issues. Our proposed sonication method for modifying natural fibers overcomes this bottleneck.

The system used for direct ink writing is shown in Fig. 3a. It was developed by modifying a dispensing robot (E3V, Nordson EFD). DIW was implemented by extruding inks through dispensing tips onto a moving platform in a trace-by-trace and layer-by-layer way. The air pressure and the vacuum level were accurately controlled by dispensers (Ultimus II, Nordson EFD). Traces were directly written using various stationary blunt stainless-steel syringe tips with inner diameters ranging from 0.10 mm to 1.37 mm and a pump system coupled with a motorized XY stage. Inks were loaded into 10 cc syringe barrels. The experimental setup also consists of a pressure controller which can regulate the ink flow rate in a pre-determined manner, a heat-controlled platform, and a CCD camera. The platform temperature was controlled and can be adjusted from 25 °C to 135 °C. The syringe tip was fixed at a Z stage. The standoff distance is proportional to the tip gauge for each experiment. A CCD camera for visually detecting such standoff distance is enabled. The CCD camera was also used to monitor the dispensing process in real time. The stage was reset to the origin point to initiate a printing job. Upon reaching the starting position of a trace, the pre-set pressure from the regulator is started immediately after the start of the platform motion. The pressure is reduced at the end of the trace. An elevated temperature of 100 °C was used during the composite ink printing, resulting in fast curing within several minutes. The thoroughly solidified composite was cooled down to room temperature after printing for further mechanical property measurements. In this study, to investigate the printability of the flax elastomer composites, we tested several stainless steel blunt dispensing tips (McMaster Carr). As shown in Fig. 3b, the inner diameters of these tips range from 0.48 mm to 1.37 mm.

2.4. Surface-modified flax elastomer composite ink characterization

In DIW process, the typical rheological requirements for the ink with good printability are: (a) shearing thinning, and (b) storage modulus/loss modulus ratio » 1 under small shear stress and ≪ 1 under large shear stress [35,36]. Requirement (a), shear-thinning behavior, easily enables

the extrusion through fine diameter dispensing tips without requiring large shear stress under high printing air pressure for high-resolution printing. While requirement (b) ensures the printed filament stays its original shape to prevent liquid instability issues such as bulging and breaking into droplets. Herein, rheological properties of the prepared 0.2 wt% and 0.5 wt% flax composite inks were measured by a rotational rheometer (Kinexus ultra+, Malvern) under a 25 mm diameter plate geometry. The plate geometry is supported by a virtually frictionless air bearing and driven by an ultra-low inertia motor, coupled to an ultra-high precision position encoder. The controllable motor torque characterized the rheological properties. Both inks in this measurement are free of curing agent to eliminate the influence of the elastomer curing. After loading into the 0.3 mm gap between the fixed substrate and the movable plate, inks were stabilized at 25 °C for 5 min. The test usually proceeds through a logarithmic sequence of shear rates while measuring the apparent viscosity at 25 °C.

As shown in Fig. 4a, the 0.5 wt% flax composite ink reveals a slight shear-thinning behavior. It has a higher apparent viscosity up to 14.1 Pa s when the shear rate ranges from 0.1 s^{-1} to 10 s^{-1}. On the other hand, the 0.2 wt% flax composite ink reveals a practically Newtonian-line behavior. The apparent viscosity of the 0.2 wt% flax composite decreases from 6.9 Pa s to 5.1 Pa s when the shear rate increases from 0.1 s^{-1} to 100 s^{-1}. Both inks reveal a similar apparent viscosity trend in the 10 s^{-1} to 100 s^{-1} shear-rate range, which ensures the printability in extrusion-based additive manufacturing technologies. Fig. 4a also shows the summary of the measured contact angles of flax/matrix inks on the glass substrate. Equilibrium contact angles of the inks were measured using a high-definition greyscale camera (CMLN-13S2M-CS, Point Grey Research Inc) with a 35 mm lens at 25 °C. Both inks reveal similar equilibrium contact angles (approximately 21°), indicating a moderate wettability of the prepared inks on a smooth surface finish. Fig. 4b shows the storage modulus (G′) and loss modulus (G′′) as functions of shear stress for the prepared 0.2 wt% and 0.5 wt% flax composite inks. Both inks are elastic-like solids (G' » G'') with respective G' values of 106.6 and 487.2 Pa that flow when their respective shear yield stress values of 0.16 and 1.59 Pa are exceeded. Once these inks exit the nozzle and return to the zero-shear conditions, they rapidly retain their filamentary shape.

In this study, the elastomer material is a polydimethylsiloxane (PDMS)-based two-component elastomer. It is heat-cured with an approximately 90 min pot life. After mixing, the material viscosity is gradually increased due to the crosslinking process. Since the fabrication process of specimens for the mechanical test can take up to 20 min, we investigated the viscosity dynamics of the elastomer under various curing temperatures, as shown in Fig. 4c. The measured apparent viscosities at a consistent 1 s^{-1} shear rate at 25 °C, 37 °C, and 50 °C are plotted. At 25 °C, the apparent viscosity (approximately 3.3 Pa s) is barely affected within the first 20 min after mixing. At 37 °C, the apparent viscosity slightly increased from 3.3 Pa s to 3.9 Pa s, the influence of the viscosity change on the printed geometry is minor. At 50 °C, the apparent viscosity increased from the 3.3 Pa s to 8.6 Pa s due to the heat-induced crosslinking process of the elastomer. To keep a uniform printed geometry accordingly, the time-dependent adjustment in printing parameter settings such as decreasing printing speed and increasing air pressure is necessary.

To characterize the printed trace geometry, 0.2 wt% surface-modified flax elastomer composites are printed using blunt dispensing tips at 5–30 mm/s printing velocity under various air pressures (1.0–5.0 psi) at room temperature. The printing substrate was glass, and the standoff distance (distance between the substrate and the dispensing tip) was 100 μm. The width of the printed trace was measured by an optical microscope (Micro-Vu SOL161), as shown in Fig. 4d, by varying the print speed, dispensing tip size, air pressure, the printed trace width can be adjusted from 0.2 mm to 4.4 mm.

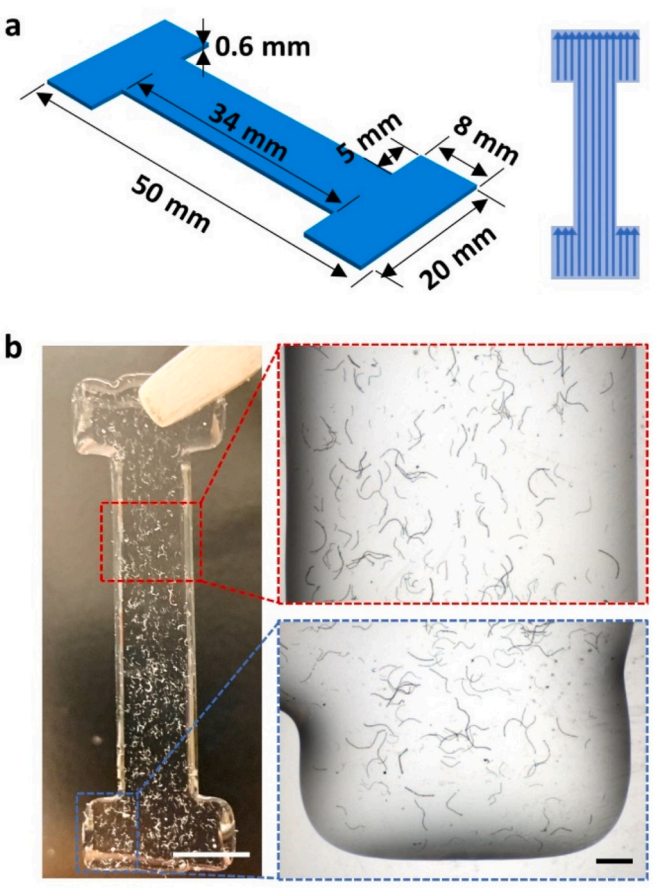

Fig. 5. Geometry and fabrication process of specimens. (a) Mechanical test specimen geometry and fabrication pattern. (b) Images of printed specimen, left scale bar = 10 mm, right scale bar = 2 mm.

2.5. Specimen geometry and manufacturing process

In this study, a single-layer sample with "I" shape geometry was designed for mechanical characterization, as shown in Fig. 5a. Traces were printed in the same direction with a 2 mm distance between each trace. To write those samples, a 1.37 mm inner diameter stainless steel tip was used to extrude inks onto a glass substrate. The standoff distance was 0.5 mm. The printing speed was 18 mm/s, and the input air pressure was 1.0 psi. The printing temperature was evaluated up to 100 °C to rapidly solidify the samples. The printed sample is shown in Fig. 5b. It was found that the surface-modified flax fibers are uniformly distributed in the PDMS matrix without agglomerations.

3. Results and discussion

3.1. Printability of surface-modified flax elastomer composites

The printability of 0.2 wt% and 0.5 wt% flax elastomer composites are experimentally characterized through various sized dispensing tips under different sonication process settings. The inner diameters of the blunt dispensing tips are 0.48 mm, 0.97 mm, and 1.37 mm, separately. To characterize the printability, the as-prepared composites are consistently extruded using 3.0 psi pressure for 120 s to determine the printability. In the repeat experiments, if the tip clogging issue happens, we consider it as a failure. The typical tip clogging issue in extrusion-based AM is caused by the fiber agglomeration, as shown in Fig. 6a. Such agglomeration is usually due to the oversized fiber bundles in the composite, which can form large fiber blocks near the joint between the dispensing tip and the syringe barrel, which leaves insufficient room for

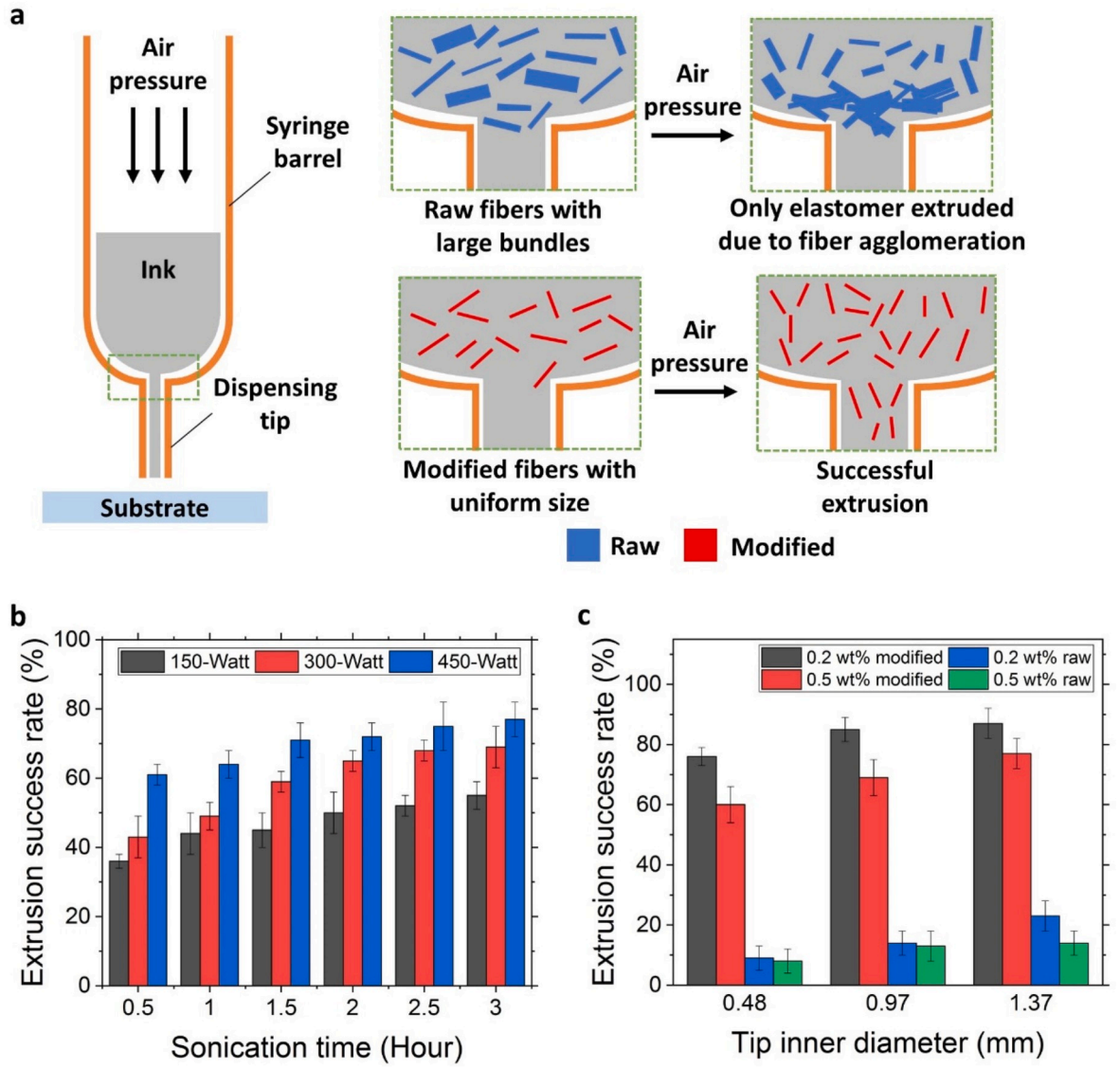

Fig. 6. Printability of surface-modified flax elastomer composites. (a) Typical fiber composites clogging issue. (b) Extrusion success rate of 0.5 wt% surface-modified flax elastomer from different sonication settings, 95% CI. (c) Extrusion success rate of 0.2 wt% and 0.5 wt% raw and surface-modified flax elastomer composites through various sized dispensing tips, 95% CI.

fiber movement, resulting in a printed trace with minimal fiber loading. The proposed sonication-based surface modification process for flax can separate those large fiber bundles, to enhance the natural fiber-based composite extrusion process.

As shown in Fig. 6b, we first investigated the influence of sonication process setting on the extrusion success rate. The inks in this test were loaded by 0.5 wt% fibers in PDMS. The test was conducted using 0.97 mm dispensing tips. The sonication power settings were 150-Watt, 300-Watt, and 450-Watt, separately. This test indicates that the sonication time is generally proportional to the extrusion success rate, while sonication time longer than 2 h shows insignificant improvement for 300-Watt and 450-Watt settings with an approximately larger than 70% extrusion success rate. The sonication power is also proportional to the extrusion success rate. 150-Watt power setting shows the least improvement in printability, while 300-Watt and 450-Watt have much higher extrusion success rate in the overall trend.

We also studied the influence of dispensing tip on the printability. Fig. 6c demonstrates the extrusion success rate of 0.2 wt% and 0.5 wt% raw and modified fiber elastomer composites after 3 h sonication process at 300-Watt power setting. As expected, surface-modified fibers show a much higher extrusion success rate. For 0.97 mm and 1.37 mm dispensing tips, the extrusion success rates of surface-modified 0.2 wt% and 0.5 wt% fiber elastomer composites are similar, range from 69% to 85%, which is almost four times of the raw fiber ones with only 13%–23% extrusion success rate. For the 0.48 mm dispensing tip, the extrusion success rate of surface-modified 0.2 wt% and 0.5 wt% fiber elastomer composites decreased to 76% and 60%, separately. This can be explained by the fiber length (0.5 mm–1.0 mm in this study), which is longer than the tip inner diameter, somehow increases the potential of clogging. The 0.5 wt% flax fiber composites have a slightly lower extrusion success rate than 0.2 wt% for all the dispensing tips. The findings in this study reveals that the sonication-based surface modification process enables the extrusion of natural fiber embedded elastomer composites.

3.2. *Mechanical properties of surface-modified flax elastomer composites*

The tensile strengths of the 0 wt%, 0.2 wt%, and 0.5 wt% surface-modified short flax fiber elastomer composites are presented in Fig. 7a. The measurements were conducted using an Instron 5942 tensile

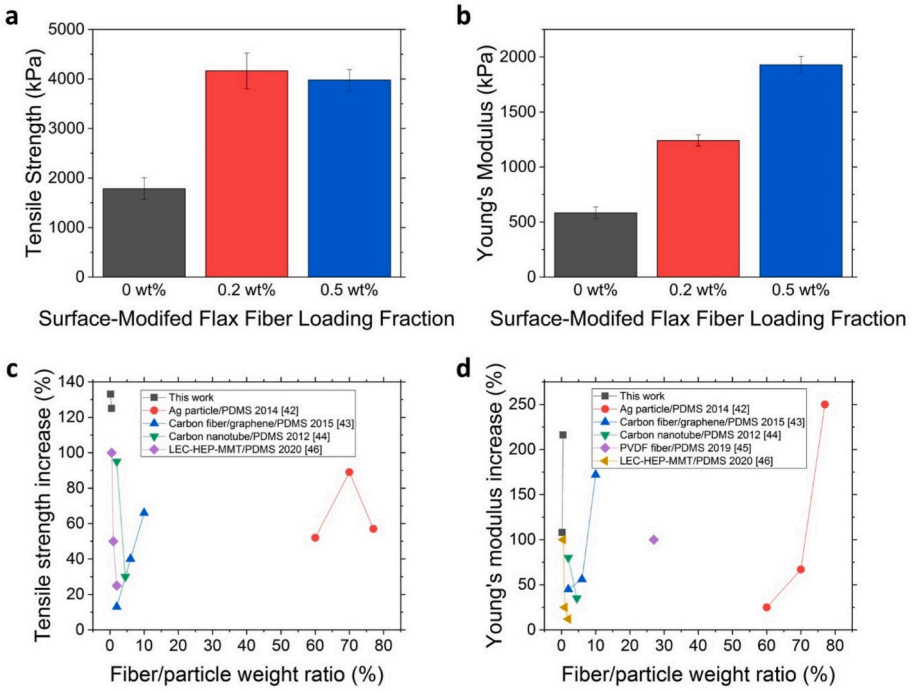

Fig. 7. Mechanical behavior of surface-modified short flax composites with different fiber loading fraction. (a) Measured tensile strength of flax elastomer composites. (b) Measured Young's modulus of flax elastomer composites. (c) Tensile strength of flax-reinforced and other synthetic fibers/particles with different loading fractions. (d) Young's modulus of flax-reinforced and other synthetic fibers/particles with different loading fractions.

tester. Both 0.2 wt% and 0.5 wt% flax elastomer composites revealed an approximately 122% increase (from 1800 kPa to 4000 kPa) in tensile strength, compared with the pure elastomer. However, when the fiber loading fraction increases from 0.2 wt% to 0.5 wt%, the tensile strength of the composite did not reveal a noticeable difference. Many studies have reported that the addition of natural and synthetic fibers is beneficial for improving the tensile strength [37–39]. However, the loading fraction was usually much higher in those studies compared to the present work, and the samples were mostly fabricated using injection molding or subtractive manufacturing approaches. For example, to achieve an approximate 100% increase in the tensile strength in the elastomer-based composite, it requires at least a 1.0 wt% carbon fiber loading fraction [40], whereas adding only 0.2 wt% of flax fibers is sufficient in the present case. The increased tensile strength is beneficial for many elastomer-based applications, including soft robotics under harsh conditions where a high bearing capability is required.

The measured Young's moduli with different fiber loading fractions are presented in Fig. 7b. The average Young's modulus increases from 580 kPa to 1250 kPa and 1860 kPa after adding 0.2 wt% and 0.5 wt% flax fibers, respectively. The increase in Young's modulus associated with the increase in fiber loading reveals a similar trend to many natural fiber-embedded polymer composites fabricated by conventional methods, such as injection molding and subtractive manufacturing [41]. However, the enhancement in stiffness in these traditional approaches arises solely from the randomly distributed fibers within the entire polymer matrix, without any local control of more complex structures. Our approach enables a spatial control of fiber distribution by varying the printing process layer-wise and partially adjusting printing pattern.

As summarized in Fig. 7c and d, both tensile strength and Young's modulus of the proposed flax elastomer composites can be adjusted by adding a much smaller amount of surface-modified short flax fibers, in comparison with many synthetic fibers and particles, e.g., such as carbon fibers, Ag particles, PVDF fibers, and low-dimensional carbon-based materials-embedded elastomer-based composites [42–46].

4. Conclusions

In this study, we reported the direct ink writing of bio-compatible surface-modified short flax elastomer composites with tunable mechanical properties. The rheological properties of ink were engineered for a smooth extrusion. The printability of the composites through various sized dispensing tips is investigated. In this work, we found that the addition of a minimal amount of short flax fibers can significantly change the mechanical performance, showing a super excellent capability in mechanical property engineering, compared to many other fiber-embedded composites reported in literature. By slightly adjusting the filler concentration, mechanical properties of the elastomer composites can be finely tuned in a wide range, providing new application opportunities in many fields including soft robotics and flexible wearable electronics. The flexibility, softness, and biocompatibility associated with the surface - modified flax fiber elastomer composites are promising. Our approach broadens the design and structural complexity for natural fiber-embedded elastomer composites.

Declaration of competing interest

The authors declare that they have no known competing financial interests or personal relationships that could have appeared to influence the work reported in this paper.

CRediT authorship contribution statement

Yizhou Jiang: Writing - original draft, Conceptualization, Methodology, Visualization, Investigation. **Jevon Plog:** Data curation, Methodology, Investigation. **Alexander L. Yarin:** Supervision, Validation, Writing - review & editing. **Yayue Pan:** Supervision, Validation, Writing - review & editing.

Acknowledgement

This material is based upon work supported by the National Science

Foundation under Grant Number (1825626). Any opinions, findings, and conclusions or recommendations expressed in this material are those of the author(s) and do not necessarily reflect the views of the National Science Foundation.

References

[1] Jo B, Van Lerberghe LM, Motsegood KM, Beebe DJ. Three-dimensional micro-channel fabrication in polydimethylsiloxane (PDMS) elastomer. J. Microelectromech. Syst. 2000;9(1):76–81.

[2] Mata A, Fleischman AJ, Roy S. Characterization of polydimethylsiloxane (PDMS) properties for biomedical micro/nanosystems. Biomed Microdevices 2005;7(4):281–93.

[3] Liu Y, Song Y, Niu S, Zhang Y, Han Z, Ren L. Integrated super-hydrophobic and antireflective PDMS bio-templated from nano-conical structures of cicada wings. RSC Adv 2016;6(110):108974–80.

[4] Morent R, De Geyter N, Axisa F, De Smet N, Gengembre L, De Leersnyder E, Leys C, Vanfleteren J, Rymarczyk-Machal M, Schacht E. Adhesion enhancement by a dielectric barrier discharge of PDMS used for flexible and stretchable electronics. J Phys D 2007;40(23):7392.

[5] Al-Saleh MH, Sundararaj U. A review of vapor grown carbon nanofiber/polymer conductive composites. Carbon 2009;47(1):2–22.

[6] Xiong J, Ma L, Wu L, Wang B, Vaziri A. Fabrication and crushing behavior of low density carbon fiber composite pyramidal truss structures. Compos Struct 2010;92(11):2695–702.

[7] Toopchi-Nezhad H, Tait MJ, Drysdale RG. Testing and modeling of square carbon fiber-reinforced elastomeric seismic isolators. Struct Contr Health Monit: The Official Journal of the International Association for Structural Control and Monitoring and of the European Association for the Control of Structures 2008;15(6):876–900.

[8] Stamhuis J. Mechanical properties and morphology of polypropylene composites. III. Short glass fiber reinforced elastomer modified polypropylene. Polym Compos 1988;9(4):280–4.

[9] Park M, Im J, Shin M, Min Y, Park J, Cho H, Park S, Shim M, Jeon S, Chung D. Highly stretchable electric circuits from a composite material of silver nanoparticles and elastomeric fibres. Nat Nanotechnol 2012;7(12):803.

[10] Orue A, Jauregi A, Unsuain U, Labidi J, Eceiza A, Arbelaiz A. The effect of alkaline and silane treatments on mechanical properties and breakage of sisal fibers and poly (lactic acid)/sisal fiber composites. Compos Appl Sci Manuf 2016;84:186–95.

[11] Matsuzaki R, Ueda M, Namiki M, Jeong T, Asahara H, Horiguchi K, Nakamura T, Todoroki A, Hirano Y. Three-dimensional printing of continuous-fiber composites by in-nozzle impregnation. Sci Rep 2016;6:23058.

[12] López Manchado M, Arroyo M, Biagiotti J, Kenny J. Enhancement of mechanical properties and interfacial adhesion of PP/EPDM/flax fiber composites using maleic anhydride as a compatibilizer. J Appl Polym Sci 2003;90(8):2170–8.

[13] Sanjay M, Madhu P, Jawaid M, Senthamaraikannan P, Senthil S, Pradeep S. Characterization and properties of natural fiber polymer composites: a comprehensive review. J Clean Prod 2018;172:566–81.

[14] Ahmad F, Choi HS, Park MK. A review: natural fiber composites selection in view of mechanical, light weight, and economic properties. Macromol Mater Eng 2015;300(1):10–24.

[15] Tan BK, Ching YC, Poh SC, Abdullah LC, Gan SN. A review of natural fiber reinforced poly (vinyl alcohol) based composites: application and opportunity. Polymers 2015;7(11):2205–22.

[16] Jost K, Durkin DP, Haverhals LM, Brown EK, Langenstein M, De Long HC, Trulove PC, Gogotsi Y, Dion G. Natural fiber welded electrode yarns for knittable textile supercapacitors. Adv. Energy Mater. 2015;5(4):1401286.

[17] Yan L, Chouw N, Yuan X. Improving the mechanical properties of natural fibre fabric reinforced epoxy composites by alkali treatment. J Reinforc Plast Compos 2012;31(6):425–37.

[18] Dewilde B. Eeuwen vlas in vlaanderen. Tielt, bussum, lannoo 20.

[19] Flax Council of Canada. http://www.flaxcouncil.ca/. Accessed 12/16/2019.

[20] International Natural Fiber Organization. http://naturalfibersinfo.org/. Accessed 12/16/2019.

[21] LIBECO. http://www.libeco.com/. Accessed 12/16/2019.

[22] Charlet K, Eve S, Jernot J, Gomina M, Breard J. Tensile deformation of a flax fiber. Procedia Eng 2009;1(1):233–6.

[23] Garkhail S, Heijenrath R, Peijs T. Mechanical properties of natural-fibre-mat-reinforced thermoplastics based on flax fibres and polypropylene. Appl Compos Mater 2000;7(5–6):351–72.

[24] Mohanty A, Khan MA, Hinrichsen G. Surface modification of jute and its influence on performance of biodegradable jute-fabric/Biopol composites. Compos Sci Technol 2000;60(7):1115–24.

[25] Mohanty S, Nayak SK. Short bamboo fiber-reinforced HDPE composites: influence of fiber content and modification on strength of the composite. J Reinforc Plast Compos 2010;29(14):2199–210.

[26] Tekinalp HL, Kunc V, Velez-Garcia GM, Duty CE, Love LJ, Naskar AK, Blue CA, Ozcan S. Highly oriented carbon fiber–polymer composites via additive manufacturing. Compos Sci Technol 2014;105:144–50.

[27] Tian X, Liu T, Yang C, Wang Q, Li D. Interface and performance of 3D printed continuous carbon fiber reinforced PLA composites. Compos Appl Sci Manuf 2016;88:198–205.

[28] Shofner M, Lozano K, Rodríguez-Macías F, Barrera E. Nanofiber-reinforced polymers prepared by fused deposition modeling. J Appl Polym Sci 2003;89(11):3081–90.

[29] Calvert P, Lin TL, Martin H. Extrusion freeform fabrication of chopped-fibre reinforced composites. High Perform Polym 1997;9(4):449–56.

[30] Frutiger A, Muth JT, Vogt DM, Mengüç Y, Campo A, Valentine AD, Walsh CJ, Lewis JA. Capacitive soft strain sensors via multicore–shell fiber printing. Adv Mater 2015;27(15):2440–6.

[31] Raney JR, Compton BG, Mueller J, Ober TJ, Shea K, Lewis JA. Rotational 3D printing of damage-tolerant composites with programmable mechanics. Proc Natl Acad Sci U S A 2018;115(6):1198–203.

[32] Huang X, Netravali A. Characterization of flax fiber reinforced soy protein resin based green composites modified with nano-clay particles. Compos Sci Technol 2007;67(10):2005–14.

[33] Amiri A, Ulven C, Huo S. Effect of chemical treatment of flax fiber and resin manipulation on service life of their composites using time-temperature superposition. Polymers 2015;7(10):1965–78.

[34] Wang X, Jiang M, Zhou Z, Gou J, Hui D. 3D printing of polymer matrix composites: a review and prospective. Compos B Eng 2017;110:442–58.

[35] Wehner M, Truby RL, Fitzgerald DJ, Mosadegh B, Whitesides GM, Lewis JA, Wood RJ. An integrated design and fabrication strategy for entirely soft, autonomous robots. Nature 2016;536(7617):451.

[36] Wei T, Ahn BY, Grotto J, Lewis JA. 3D printing of customized li-ion batteries with thick electrodes. Adv Mater 2018;30(16):1703027.

[37] Yuan X, Zhang Y, Zhang X. Maleated polypropylene as a coupling agent for polypropylene–waste newspaper flour composites. J Appl Polym Sci 1999;71(2):333–7.

[38] Fu S, Lauke B, Mäder E, Yue C, Hu X. Tensile properties of short-glass-fiber-and short-carbon-fiber-reinforced polypropylene composites. Compos Appl Sci Manuf 2000;31(10):1117–25.

[39] Ramesh M, Palanikumar K, Reddy KH. Plant fibre based bio-composites: sustainable and renewable green materials. Renew Sustain Energy Rev 2017;79:558–84.

[40] Tibbetts GG, McHugh JJ. Mechanical properties of vapor-grown carbon fiber composites with thermoplastic matrices. J Mater Res 1999;14(7):2871–80.

[41] Ku H, Wang H, Pattarachaiyakoop N, Trada M. A review on the tensile properties of natural fiber reinforced polymer composites. Compos B Eng 2011;42(4):856–73.

[42] Corbaci M. Implementation of soft lithography for the fabrication of stacked dielectric elastomer actuators for soft robotics. 2018.

[43] Zhao Y, Zhang Y, Bai S, Yuan X. Carbon fibre/graphene foam/polymer composites with enhanced mechanical and thermal properties. Compos B Eng 2016;94:102–8.

[44] Jung H, Moon J, Baek D, Lee J, Choi Y, Hong J, Lee S. CNT/PDMS composite flexible dry electrodesfor long-term ECG monitoring. IEEE (Inst Electr Electron Eng) Trans Biomed Eng 2012;59(5):1472–9.

[45] Nguyen DN, Moon W. Fabrication and characterization of a flexible PVDF fiber-based polymer composite for high-performance energy harvesting devices. J Sensor Sci Technol 2019;28(4):205–15.

[46] Meng N, Zhang M, Ge MQ, Zhou N, Chi C, Chu X, et al. Montmorillonite-lecithin-heparin/PDMS films with enhanced mechanical and antithrombogenic properties. Polym Compos. https://doi-org.proxy.cc.uic.edu/10.1002/pc.25513.